Grain-Boundary Effect on Low-Field Magnetoresistance in Perovskite Manganites

Yunhui XU
Institute of Experimental Physics, University of Saarbrücken, Building 22,
66041 Saarbrücken, Germany

Research results on perocskite manganite materials and bulk sensors are reported. Magnetic field sensors from bulk $La_{0.67}Ca_{0.33}MnO_3$, $La_{0.67}Sr_{0.33}MnO_3$ and $La_{0.67}Ba_{0.33}MnO_3$ were fabricated and characterized at fields of 0 - 8 Tesla and temperatures of 4.2 - 300 K. The sensors exhibit nearly linear response and are fairly field-sensitive at high fields. A particularly large magnetoresistance (MR) is observed at low fields. This low-field MR is found to be highly anisotropic. Possible effects of grain-boundaries (GB) on the low-field MR are discussed. An explanation of the anisotropy of low-field MR is proposed.

Key words: colossal magnetoresistance (CMR); perovskite manganites; grain boundaries (GB).

INTRODUCTION

Very large magnetoresistance (MR), $\Delta R/R_H = (R_H-R_0)/R_H$, (where R_H and R_0 are the resistance under field H and zero field, respectively), of up to 10^7 % under fields of several Tesla has been obtained in perovskite manganites $A_{1-x}B_xMnO_3$, where A is a trivalent rare-earth element and B is a divalent alkali-earth element. The MR is most pronounced in the vicinity of the ferromagnetic ordering temperature (Curie-temperature) T_C [1-3]. The metallic and ferromagnetic state of the doped manganites is usually explained by the double-exchange model based on the exchange of electrons between Mn^{3+} and Mn^{4+} ions[4]. This intrinsic high-field MR, known as colossal magnetoresistance (CMR), is due to field-induced suppression of spin fluctuations. Although the high MR ratio is technologically promising, the field needed to generate such colossal MR effects is too high for most applications. Recently, a large low-field MR over a wide temperature range from 4.2 K up to T_C has been discovered for sintered bulk samples and polycrystalline films [5-11]. Typical values are, e.g., 6-25 % at 200-4.2 K and zero field (extrapolated) for $La_{2/3}Sr_{1/3}MnO_3$[5], and over 3% at 2 mT and 300 K for $La_{0.7}Sr_{0.3}MnO_3$[11]. These values are much larger than the $\Delta R/R_H$ value of 2% for permalloy. This extrinsic low-field MR has been attributed to the effects of grain boundaries (GB)[5-11]. The low-field MR is quite interesting for both fundamental understanding and potential sensor applications of these materials. Apart from high $\Delta R/R_H$ values at low field and over a wide temperature range, chemical stability, adjustable T_C, straightforward synthesis, and low production costs make polycrystalline perovskite materials very competitive in the field of magnetoresistive applications.

This paper reports the measurements on $La_{0.67}Ca_{0.33}MnO_3$, $La_{0.67}Sr_{0.33}MnO_3$, and $La_{0.67}Ba_{0.33}MnO_3$ polycrystalline sensors. Field sensitivities as high as -200 %/T at 1-3 mT and 294 K, -900 %/T at 3-8 mT and 75 K, and -1000 %/T at 1-3 mT and 4.2 K were obtained. The low-field MR is found to be highly anisotropic. The effects of GBs on the transport property at low-field are discussed. An explanation of the anisotropy of the low-field MR is proposed and the reason why it can not be simply attributed to a demagnetization effect is discussed.

EXPERIMENTAL RESULTS AND DISCUSSION

Ceramic samples of $La_{0.67}Ca_{0.33}MnO_3$, $La_{0.67}Sr_{0.33}MnO_3$, and $La_{0.67}Ba_{0.33}MnO_3$, were prepared by solid-state reaction. Stoichiometric amounts of high-purity La_2O_3, $CaCO_3$, $BaCO_3$, $SrCO_3$, and Mn_2O_3 were thoroughly mixed, ground, and repeatedly preheated in air at 1090°C for 48 h and reground. Finally, the fine powders were cold-pressed into pellets at 13-18 kN/cm², and sintered at 1400 °C for 12 h. XRD measurements revealed that all samples are single perovskite phase. SEM image showed a clear polycrystalline structure with grain sizes between a few nm and ~10 µm. The Curie temperatures determined at the ferromagnetic transition are 268 K, 365 K and 348 K for $La_{0.67}Ca_{0.33}MnO_3$, $La_{0.67}Sr_{0.33}MnO_3$, and $La_{0.67}Ba_{0.33}MnO_3$, respectively.

The bulk samples were cut into about 8x0.8x0.14 mm^3 thin stripes by a fine diamond saw and capsulated together with four electrical leads on a Al_2O_3 carrier[12,13]. The resistance of the sensors was measured using the four-point method under fields of 0 to 8 T at 4.2 K, 75 K and room temperatures. Offset voltages were subtracted by reversing the current. For all sensors the current **J** is applied along their long axis. The resistance is measured under a field **H** along the three axes with respect to

the long axis: longitudinal $R_{//}$ (**H**//**J**), transverse R_T (in-plane field, normal to **J**), and perpendicular $R_\perp$ (field perpendicular to the sample plane).

The field dependence of the resistance for the $La_{0.67}Sr_{0.33}MnO_3$ and $La_{0.67}Ba_{0.33}MnO_3$ sensors at 292.5 K is shown in Fig. 1. The resistance values for increasing and decreasing field are identical. The MR thus does not exhibit hysteresis for both $R_{//}$ (circles) and R_T (triangles). The R(H) curves exhibit a linearity of about 0.8 for $La_{0.67}Sr_{0.33}MnO_3$ (ratio of the sensitivities at 7 T and 1 T). The sensitivity of about 0.08 Ω/T at high fields and room temperature can also be derived from Fig. 1. A sharp drop of $R_{//}$ is observed at low field followed by the overall decrease at higher fields. This sharp drop is not observed for R_T. Note that the $R_{//}$ values are lower than the R_T values by about 0.02 Ω. This is believed to be due to the cumulative effect of the anomalous low-field sensitivity along the long axis of the sensor. For the $La_{0.67}Ca_{0.33}MnO_3$ sample at room temperature (above its T_C, 268 K) no pronounced low-field drop of both $R_{//}$ and R_T is observed. This clearly indicates that the low-field behavior is related to ferromagnetic ordering below T_C.

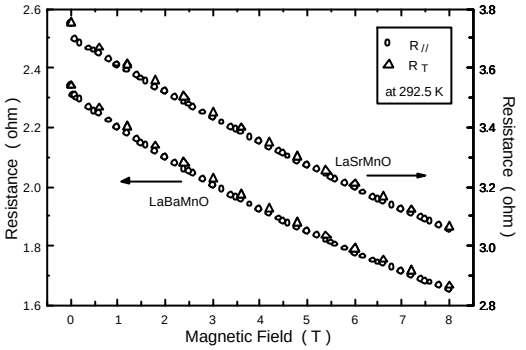

Figure 1. Field dependence of the ohmic resistance of $La_{0.67}Sr_{0.33}MnO_3$ and $La_{0.67}Ba_{0.33}MnO_3$ thin samples at 292.5 K. The circles and triangles represent the longitudinal (**H**//**J**) and transverse (**H** oriented in the sample plane, perpendicular to **J**) resistance $R_{//}$ and R_T, respectively. There is a pronounced drop of $R_{//}$ but not of R_T at low field.

The dependence of the field sensitivity, defined as $S=(1/R_0)(\Delta R/\Delta H)$, on the magnetic field for $La_{0.67}Sr_{0.33}MnO_3$ and $La_{0.67}Ba_{0.33}MnO_3$ sensors at room temperature is depicted in Fig. 2. An anomalously large sensitivity is seen near zero field for the parallel case, but is not seen for the transverse and perpendicular cases. At higher fields (H≥3T), however, the sensitivities at longitudinal, transverse and perpendicular fields become the same (about -4 %/T) and thus exhibit an isotropic behavior.

The low-field MR is highly anisotropic and most pronounced when the field is applied along the long axis. In this case the slope ΔR/ΔH maxima are 6 Ω/T at a field of 3 mT and at 298 K, and 12-15 Ω/T at 3-8 mT and at 77 K[12,13]. This ΔR/ΔH is high enough to fabricate useful magnetic devices which can compete favorably with existing ones. For example, compared with 8 mV/T at a recommended current of 100 mA (corresponding to 0.08 Ω/T) for some commercial sensors[14], the low-field ΔR/ΔH of the present manganite sensors are clearly superior. R_T decreases only slightly with increasing field. For $R_\perp$ no change can be detected up to 15 mT [12,13]. In the parallel case, low-field sensitivities $S_{//}$, as high as -200 %/T at 1-3 mT and 294 K, -900 %/T at 3-8 mT and 75 K, and -1000 %/T at 1-3 mT and 4.2 K were obtained. The low-field S_T and $S_\perp$ maxima in figure 2 at room temperature are -10 %/T at 3-5 mT and -6 %/T at 60-80 mT, respectively. This anisotropic response can not be simply attributed to a demagnetization effect. This will be discussed later.

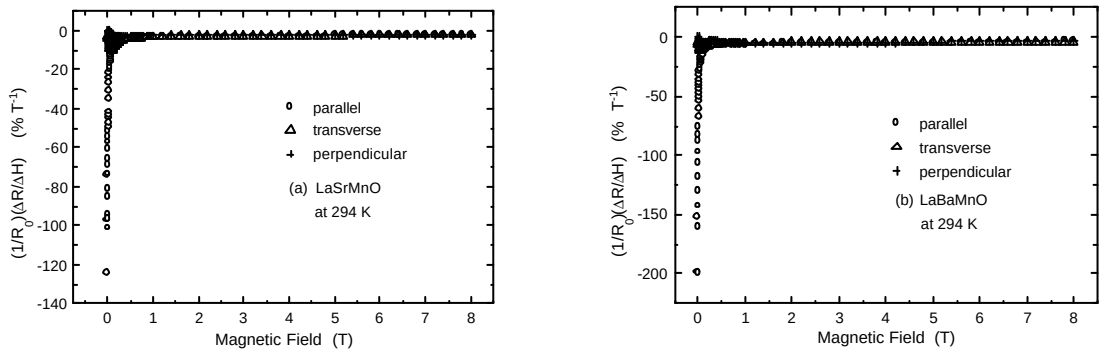

Figure 2. Dependence of field sensitivity, $S=(1/R_0)(\Delta R/\Delta H)$, on the magnetic field at room temperature for (a) $La_{0.67}Sr_{0.33}MnO_3$ and (b) $La_{0.67}Ba_{0.33}MnO_3$ sensors. The circles represent longitudinal sensitivity $S_{//}$, the triangles - transverse S_T, and the crosses - perpendicular $S_\perp$ contributions. The largest sensitivity, as high as -200 %/T is found at low fields for **H**//**J**.

For further exploring of the low-field behavior, figure 3 shows a detailed dependence of both normalized resistance R/R_0 (upper) and normalized magnetization M/M_{2T} (lower) on the magnetic field of three directions for $La_{0.67}Sr_{0.33}MnO_3$ at room temperature. The sample dimensions are 8x0.8x0.14 mm^3 for resistance measurement (upper) and 5x0.8x0.14 mm^3 for magnetization measurement in a vibrating sample magnetometer (lower). A sharp drop of R/R_0 at low-field is presented and „saturated" at a certain field H_s. The „saturation" field H_s of the low-field MR is determined as the field, at which the extrapolated line of the high-field MR intersects with the low-field MR curve. The values of $H_{s(MR)}$ of low-field MR, derived from Fig. 3 upper panel, are: $H_{s(MR)//}$=0.033 T, $H_{s(MR)T}$=0.13T, and $H_{s(MR)\perp}$=0.18T, for three orientations of the field respectively. The values of the saturation field of magnetization $H_{s(M)}$, derived from Fig. 3 lower panel, are much higher than $H_{s(MR)}$: $H_{s(M)//}$=0.2T, $H_{s(M)T}$=0.33T, and $H_{s(M)\perp}$=0.53T, respectively. Therefore it seems that there is no direct correlation between the saturations of low-field MR and magnetization.

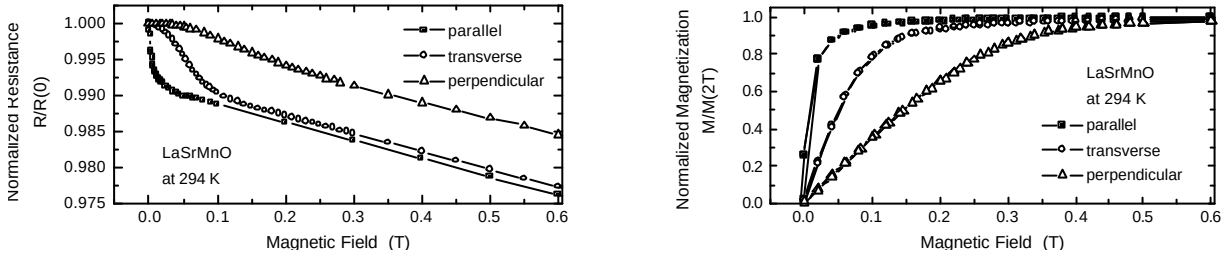

Figure 3. A comparison between the saturation fields H_s of magnetoresistance and magnetization for $La_{0.67}Sr_{0.33}MnO_3$ stripes at room temperature and for different orientations of fields.

The low-field MR is clearly associated with the properties of grain boundaries due to the following experimental corroborates: (1) The large low-field MR was observed only in sintered samples and polycrystalline thin films, not in the single crystals [5] and epitaxial films [6,8,10]. (2) It was observed only in the meander film stripe with 11 crossings of a 36.8° GB, not in stripe-shaped film without crossing of the GB[9]. (3) MR increases with decreasing particle size, indicating a substantial contribution from the grain boundaries[7]. (4) The GB-resistance and its magnetic field dependence vary strongly with the misorientation angles at the GB[11].

The mechanism of the GB-induced MR is not yet clear, although some models have been proposed. One of the models attributes the enhanced MR to spin-polarized tunneling through grain boundaries[5]. The spin-polarized tunnel resistance change can be written as $\Delta R/R=2PP'/(1+PP')$, where P and P´ are the conduction-electron spin polarization on both sides of the GB (see Ref. 5 and references herein). The other model suggests that this behavior is due to excess scattering induced by spin-disorder and structure-disorder at or near the GB-regions[6,10]. Except these two models it was also suggested that spin-polarized tunneling and spin scattering at interfaces play a relative minor role and that the dominant low-field contribution to the MR stems from the mesoscale response of magnetic inhomogeneities induced by the GB[11,15].

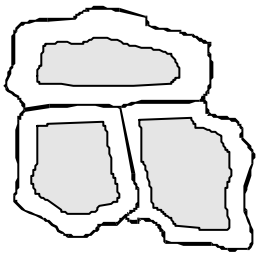

Figure 4. A schematic description of the GB regions. The gray areas present homogeneous perovskite manganites. The white areas are boundary-regions between grains, where structural distortions, stoichiometric deviations, crystal-orientation-mismatches, oxygen deficiencies, strains, and other defects are supposed to exist.

Recent research results suggest that the grain boundaries are generally expected to have stoichiometric deviations, oxygen deficiencies, crystal-orientation-mismatches, structural distortions, magnetic inhomogeneities, strains, or other defects, such as, surfaces, clusters, sub-grain boundaries, etc. Figure 4 displays a schematic picture of GB regions. The central gray areas present homogeneous ferromagnetic perovskite manganite. The white areas are the GB regions. These GB regions could be non-magnetic or weak-magnetic due to the existence of defects. For example, a strain contour from a 5° tilt GB may extend 4.4 nm from GB[15]. One percent strain results in a ΔT_C of 10 K. This disturbance increases with increasing GB angle. In asymmetric GB oxygen content variations extend several nm from GB[15]. Small change in oxygen content results in a ΔT_C of 15 K[15]. These in turn result in strong variation of local T_C and magnetization over several nm on each side of a GB. The response to magnetic field from these mesoscale regions of depressed magnetic order forms the main contribution to the low-field MR.

The anisotropic low-field response observed in this work can not be simply attributed to a demagnetization effect. The sintered polycrystalline material involves large number of grains, grain-boundaries, and even some percent of pores. These grains are randomly shaped, oriented, and separated by the GB regions of depressed magnetic order (and even by some pores as well). The macroscopic demagnetization factor for the sample of discontinuing material may differ from that for the sample of continuing medium. It was pre-assumed in a previous model[12] that the randomly oriented homogeneous regions in central part of grains are shaped spherically. Each such sphere has a demagnetization factor of 1/3 in any direction of field. The spin-alignment in GB regions was affected by both the external applied field and the internal stray field of magnetically charged grains. The anisotropy of low-field MR was then explained by assuming the existence of two extremes of GB environments under the influence of the external magnetic field: One category exhibits field-dependent resistance, while the other one is field insensitive due to local-field compensation by internal stray fields. The anisotropy of the geometry of the sample determines the ratio of the two types of GB under a field, thus determines the anisotropy of low-field MR[12].

In summary sensors from bulk perovskite manganites have been fabricated. The sensors exhibit nearly linear response and are fairly field-sensitive at high fields. A particularly large MR is observed at low fields. It is found that the high-field MR is independent of field orientation with respect to the three axes of the sensor. The low-field MR, however, is strongly anisotropic. The possible effects of grain-boundaries on the low-field MR is discussed. An explanation of the anisotropy of the low-field MR is proposed and the reason why it can not be simply attributed to a demagnetization effect is discussed.

ACKNOWLEDGMENT

The author thanks Prof. U. Hartmann of Saarbrücken University for the support to this work.

References

1. G.H. Junker and J.H. van Santen, Physica **16**, 337 (1950); G.H. Junker, Physica **22,** 707 (1956); F. O. Wollan and W. C. Koehler, Phys. Rev. **100,** 545 (1955)
2. R. von Helmolt, J. Wecker, B. Holzapfel, L. Schultz, and K. Samwer, Phys. Rev. Lett. **71,** 2331 (1993); S. Jin, T.H. Tiefelk, M. McCormak, R.A. Fastnacht, R. Ramesh, and L.H. Chen, Science **264,** 413 (1994).
3. A.P. Ramirez, J. Phys.: Condens. Matter **9**, 8171 (1997).
4. C. Zener, Phys. Rev. **82,** 403 (1951); P.W. Anderson and H. Hasegava, Phys. Rev. **100,** 675 (1955); P.-G. de Gennes, Phys. Rev. **118,** 141 (1960).
5. H.Y. Hwang, S.-W. Cheong, N.P. Ong, and B. Batlogg, Phys. Rev. Lett., **77,** 2041 (1996).
6. A. Gupta, G.Q. Gong, Gang Xiao, P.R. Duncombe, P. Lecoeur, P. Trouilloud, Y.Y. Wang, V.P. Dravid, and J.Z. Sun, Phys. Rev. B **54,** R15629 (1996).
7. R. Mahesh, R. Mahendiran, A.K. Raychaudhuri, and C.N.R. Rao, Appl. Phys. Lett. **68,** 2291 (1996).
8. R. Shreekala, M. Rajeswari, K. Ghosh, A. Goyal, J.Y. Gu, C. Kwon, Z. Trajanovic, T. Boettcher, R.L. Greene, R. Ramesh, and T. Venkatesan, Appl. Phys. Lett. **71,** 282 (1997).
9. K. Steenbeck, T. Eick, K. Kirsch, K. O´Donnell, and E. Steinbeiß , Appl. Phys. Lett. **71,** 968 (1997).
10. J.Y. Gu, S.B. Ogale, M. Rajeswari, T. Venkatesan, R. Ramesh, V. Radmilovic, U. Dahmen, G. Thomas, and T.W. Noh, Appl. Phys. Lett. **72,** 1113 (1998).
11. S.P. Isaac, N.D. Mathur, J.E. Evetts, and M.G. Blamire, Appl. Phys. Lett. **72,** 2038 (1998).
12. Yunhui Xu, V. Dworak, A. Drechsler, U. Hartmann, Appl. Phys. Lett. **74,** 2513 (1999).
13. Yunhui Xu, S. Lukas, U. Memmert, U. Hartmann, submitted to J. Phys. D: Applied Physics.
14. Bell Sensors BHA 921 and BHT 921.
15. J.L. Evetts, M.G. Blamire, N.D. Mathur, S.P. Isaac, B.-S. Teo, L.F. Cohen, and J.L. Macmanus-Driscoll, Phil. Trans. R. Soc. Lond. A **356,** 1593 (1998).